

Electrochemical Growth of Ag₂S on Ag(111) Electrodes. Coulometric and X-ray Photoelectron Spectroscopic Analysis of the Stepwise Formation of the First and Second Monolayers of Ag₂S

Jodie L. Conyers, Jr. and Henry S. White*

Department of Chemistry, University of Utah, Salt Lake City, Utah 84112

Received: October 30, 1998; In Final Form: January 11, 1999

Stepwise electrochemical growth of the first and second monolayers of Ag₂S at a Ag(111) electrode in aqueous hydrosulfide (HS[−]) solutions is reported. The deposition of the first and second monolayers occurs at different electrode potentials and can be resolved in voltammetric experiments prior to the formation of a bulk Ag₂S layer. Oxidative formation of the first Ag₂S monolayer occurs by a kinetically facile two-electron, two-step mechanism, involving the one-electron oxidative adsorption of HS[−] ($\text{Ag} + \text{HS}^- \rightleftharpoons \text{Ag-SH} + e^-$) followed by a one-electron oxidative phase transition to yield a complete Ag₂S monolayer ($\text{Ag-SH} + \text{Ag} + \text{OH}^- \rightleftharpoons \text{Ag}_2\text{S} + \text{H}_2\text{O} + e^-$). An irreversible wave corresponding to the formation of a second monolayer of Ag₂S in a single two-electron step ($2\text{Ag} + \text{HS}^- + \text{OH}^- \rightleftharpoons \text{Ag}_2\text{S} + \text{H}_2\text{O} + 2e^-$) is voltammetrically resolved at slow scan rates (<25 mV/s). Coulometric analysis of the voltammetric data demonstrates that the quantity of electricity (~164 $\mu\text{C}/\text{cm}^2$) consumed during the formation of the first and second monolayers is identical. X-ray photoelectron spectroscopy is used to monitor the surface coverage of sulfur as a function of the electrode potential during the successive deposition of the Ag-SH adlayer, the first Ag₂S monolayer, and the second Ag₂S monolayer.

Introduction

We wish to report the stepwise electrochemical formation of the first and second monolayers of Ag₂S at a Ag(111) surface. The growth of nanometer-thick films comprising a metal cation and charge-balancing anion, $\text{M}^{z+}\text{A}^{z-}$, e.g., metal oxides and sulfides, is of general interest in chemical sciences and technology. Such films are used as passive barriers to prevent corrosion, serve as active components of microelectronic devices, and are used as model systems for studying heterogeneous catalysis. Understanding the chemical and electronic properties of these films during the initial stages of growth is an important step in unraveling the fundamental structure–activity relationships of these materials. In this report, we demonstrate that the free energies of formation of the first and second monolayers of Ag₂S on Ag(111) are significantly different, and directly measurable by voltammetric methods. The difference in the energetics of these surface structures is of fundamental interest and, in addition, provides a simple means to control the thickness of the Ag₂S layer during the early stages of film growth. Specifically, we demonstrate that voltammetric methods may be used to deposit the first monolayer, a second monolayer, or a bulk film (>3 layers) of Ag₂S at the Ag(111)/solution interface.

The electrochemical formation of $\text{M}^{z+}\text{A}^{z-}$ films on a surface of metal (M) that is immersed in a solution containing the anion (A^{z-}) has been extensively studied over many years.¹ However, the details of film growth are generally not well understood, especially during the deposition of the first few monolayers. The first step in the growth of these films frequently involves the *oxidative adsorption* of anions from the solution onto the metal surface. For instance, the well-known oxidative adsorption of halides, such as Cl[−], at Ag(111) yields a layer of strongly

adsorbed ions at the Ag surface prior to the deposition of multiple molecular layers of AgCl.² The formation of a strongly adsorbed monolayer of anions is analogous to the underpotential deposition (UPD) of a foreign metal monolayer onto a metal surface prior to bulk deposition. In essence, formation of the Cl adlayer at the Ag(111)/solution interface represents the first step in the growth of a bulk AgCl film. Clearly, the structure and chemical properties of this adlayer may be quite different than that of the bulk film. During the adsorption process, partial charge transfer between Cl[−] and the Ag(111) surface results in the flow of a measurable current, which can be detected by sensitive electrochemical methods. In many instances, including Cl[−] adsorption at Ag(111), the deposition of the first anion adlayer is energetically more favorable than formation of the bulk material.² In such cases, anion adsorption can be detected in voltammetric experiments as a small prewave prior to the formation of the bulk film (i.e., at electrode potentials negative of the standard potential of the $\text{M}/\text{M}^{z+}\text{A}^{z-}$ redox couple).³

In previous studies, we have investigated the formation of the first monolayer of Ag₂S on the (111), (110), and (100) faces of Ag single-crystal electrodes.^{4,5} The Ag₂S monolayer is deposited at room temperature in aqueous solutions (pH ~ 13) containing millimolar concentrations of HS[−]. Our conclusions, based primarily on voltammetric and electrochemical quartz crystal microbalance measurements, suggest that the formation of the first Ag₂S monolayer proceeds through a two-step, two-electron mechanism. The initial step involves the one-electron oxidative adsorption of HS[−] at the Ag surface to form an adlayer of HS[−], indicated hereinafter as Ag-SH. This adlayer is further oxidized at more positive electrode potentials in a second one-electron step to yield the first monolayer of Ag₂S.⁶ Aloisi et al.⁷ have employed in situ scanning tunneling microscopy to investigate this system and have reported a $(\sqrt{7} \times \sqrt{7})\text{R}19^\circ$

* Author to whom correspondence should be addressed.

structure for the Ag₂S monolayer at the Ag(111) surface. However, their proposed mechanism differs from ours in that they suggest that the Ag₂S monolayer is formed in a *single* two-electron step without proceeding through an intermediate Ag–SH adlayer. Regardless, all previous descriptions of Ag₂S deposition at Ag(111) have been limited to the growth of a single monolayer or bulk layer. Rarely can one resolve voltammetric surface waves corresponding to the formation of a second or third monolayer of a M^{z+}A^{z-} film, as the energetics of these successive layers are not sufficiently different from that of the bulk material. In contrast, many examples of the UPD of metals exist where *multiple* monolayers are energetically resolved prior to bulk deposition of the foreign metal (e.g., Ag on Pt,⁸ Ag on Au,⁹ Tl on Au¹⁰).

In this paper, we demonstrate that the electrochemical formation of the first *and* second monolayers of Ag₂S at a Ag(111) electrode occurs in a stepwise fashion. The free energies of formation are sufficiently different that the depositions of the first and second monolayers proceed at different electrode potentials. To our knowledge, and for reasons that are not clearly understood, the ability to resolve the sequential formation of multiple monolayers of a M^{z+}A^{z-}-type film is limited to studies at liquid Hg¹¹ and amalgam electrodes.¹² For example, the successive formation of the first four molecular layers of HgS at a stationary Hg electrode is characterized by a series of four well-resolved peaks in voltammetric experiments.¹³ In addition, a few examples exist in which the successive formation of multiple layers on liquid electrodes can be resolved temporally (e.g., while monitoring the *i*–*t* response during film growth^{14,15}), but not energetically.

Experimental

Electrode Preparation. Highly oriented Ag(111) films were epitaxially grown on muscovite mica using a previously reported procedure.¹⁶ Characterization of the films by X-ray diffraction, scanning tunneling microscopy, and underpotential deposition has been reported.¹⁶ Prior to use, the Ag(111) electrodes were flame-annealed by heating the front side for several seconds using a butane micro-torch (Blazer). Studies of anion adsorption (e.g., halides,^{2f} alkanethiolates,¹⁷ polyborate,¹⁸ oxyanions,^{2f} and hydrosulfide^{4,5}) at these Ag(111) films have been reported.

Electrochemical Apparatus. A standard one-compartment, three-electrode cell equipped with an inlet port for N₂ flow was used for electrochemical measurements. All solutions were purged for ~30 min with N₂ to remove dissolved O₂ and a positive pressure of N₂ was maintained over the solutions during voltammetric measurements. A Pt wire and Ag/AgCl (3 M NaCl) electrode were employed as the auxiliary and reference electrodes, respectively. A Bioanalytical Systems (BAS) model CV-27 potentiostat was used to obtain voltammetric data at 25 ± 2 °C.

Chemicals. Reagent grade water from a Barnstead “E-pure” water purification system was used for all solutions. NaOH (Fisher Scientific, 98.1%) and Na₂S (Aldrich, 98%) were used as received.

X-ray Photoelectron Spectroscopy. XPS analysis was performed using a VG ESCA Lab multi-technique surface analysis system with Al-Kα radiation of 1486.7 eV and a base pressure of 10^{–8} Torr. High-resolution spectra were recorded in the constant analyzer energy mode with a pass energy of 20 eV. The binding energy scale was calibrated with respect to the C 1s binding energy of 284.6 ± 0.1 eV.

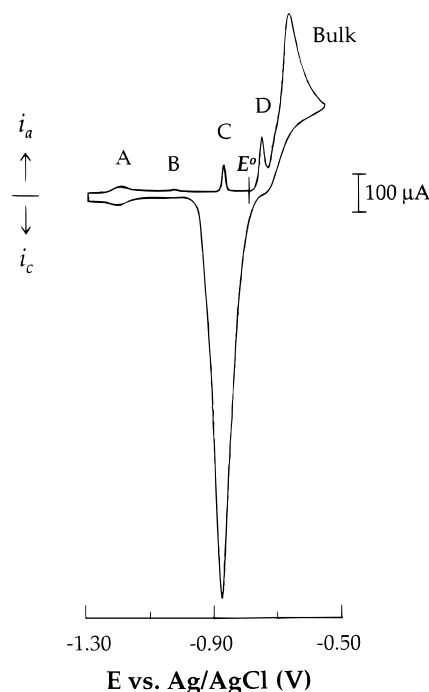


Figure 1. Voltammetric response of a flame-annealed Ag(111) electrode (area = 1.03 cm²) in a 0.2 M NaOH solution (pH = 13.3) containing 1 mM Na₂S. The predominant sulfur species in solution is HS[–] (>99.99%). Scan rate = 20 mV/s.

Results and Discussion

The cyclic voltammetric response of a Ag(111) electrode in a 0.2 M NaOH solution (pH = 13.3) containing 1 mM Na₂S is shown in Figure 1. Based on literature pK_a values for H₂S (~7.1) and HS[–] (~16.9),¹⁹ the primary S species (>99.99%) in this solution is hydrosulfide, HS[–]. The standard potential for the Ag/Ag₂S system, E⁰ = –0.775 V vs Ag/AgCl (3 M NaCl),²⁰ is labeled on the voltammetric curve in Figure 1 as a point of reference in discussing the energetics of various surface reactions. The large anodic wave at potentials positive of E⁰ (labeled “bulk”) corresponds to the formation of a relatively thick layer (~15 monolayers) of Ag₂S, as determined by coulometric and XPS analysis described below. The large cathodic wave at potentials negative of E⁰ corresponds to the reductive stripping of the bulk Ag₂S layer. On the basis of the substantial anodic and cathodic peak splitting (~0.3 V), the deposition and stripping of a thick Ag₂S layer is clearly a kinetically slow process.

Inspection of Figure 1 reveals several small voltammetric features that suggest that HS[–] is oxidatively adsorbed at the Ag(111) surface prior to the deposition of the bulk Ag₂S film. Specifically, four small waves (labeled as A, B, C, and D) are observed at potentials negative of the formation of bulk Ag₂S. These smaller waves can be cleanly resolved and characterized by adjusting the anodic switching potential, as shown in Figure 2, parts b and c. To verify that these waves are associated with the adsorption of HS[–], the voltammetric response of the same Ag(111) electrode was recorded in a 0.2 M NaOH solution in the absence of any HS[–] (Figure 2a). The voltammetric response in this “blank” solution is featureless, corresponding solely to the capacitive charging of the Ag(111)/solution interface.

Previous investigations in our laboratory^{4,5} have assigned waves A and B to the reversible adsorption of a HS[–] monolayer, (eq 1).



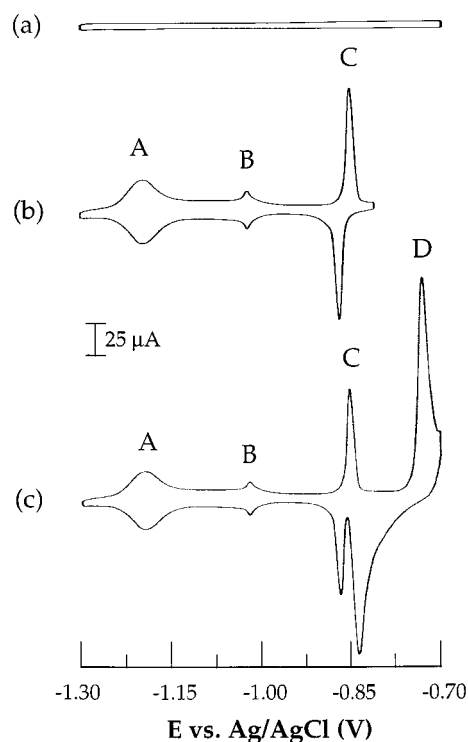
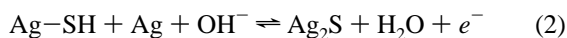
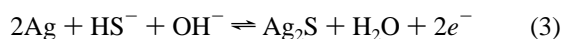


Figure 2. Voltammetric response of a flame-annealed Ag(111) electrode in an aqueous solution containing 0.2 M NaOH and 1 mM Na₂S. The voltammogram recorded in a blank solution containing only 0.2 M NaOH is shown in part (a). The voltammograms shown in (b) and (c) differ only in the value of the positive switching potential. The same electrode was used to record all three voltammetric curves (area = 0.89 cm²) at a scan rate of 20 mV/s.

Coulometric data support this interpretation; the electrical charge obtained by integration of the first two voltammetric waves is consistent with the value expected for the formation of a stoichiometrically complete adlayer of Ag–SH ($\theta \sim 0.5$).⁵ In addition, in situ EQCM data indicate that the amount of mass adsorbed over the potential range encompassing waves A and B is consistent with the formation of a monolayer of Ag–SH, $(1.19 \pm 0.16 \times 10^{-9} \text{ mol/cm}^2)$.⁵ Wave C has been assigned to the oxidation of the Ag–SH monolayer to yield a Ag₂S monolayer (eq 2).



Equation 2 represents a potential-dependent surface phase transition in which the Ag–SH adlayer is converted into the first molecular monolayer of Ag₂S, a reaction that does not involve additional adsorption of HS[−]. In situ EQCM measurements⁵ indicate that the interfacial mass does not significantly change over the potential region of wave C, consistent with eq 2. (The mass change due to the H⁺ transfer is negligibly small and is therefore not detected.) In summary, the three-wave voltammetric response (i.e., waves A, B, and C) for the formation of the Ag₂S monolayer, Figure 2b, may be characterized as a two-step, two-electron process. The overall reaction is obtained by combining eqs 1 and 2, yielding



Aloisi et al.⁷ have recently studied the formation of the first monolayer of Ag₂S at Ag(111) and have observed a small wave appearing between waves A and B. This wave is also observed in our laboratory when using Ag(111) surfaces that are not

completely annealed. If the electrode is removed from solution and annealed using a butane micro-torch, the extraneous wave disappears and the voltammogram in Figure 2b is obtained. On the basis of their interpretation of STM images obtained in situ during the voltammetric experiment, as well as coulometric analysis, Aloisi et al.⁷ have proposed that the Ag₂S monolayer is deposited continuously over the entire voltammetric region (waves A, B, and C). This mechanism is different from that described above in which an intermediate Ag–SH structure, eq 1, precedes the formation of the Ag₂S monolayer, eq 2. Later in this article, we present XPS data that support the mechanism involving a surface phase transition between the Ag–SH adlayer and the Ag₂S monolayer.

In a previous study,⁴ we had briefly described a small shoulder on the rising part of the large “bulk” Ag₂S wave, Figure 1. This partially resolved wave was tentatively associated with the formation of a second monolayer of Ag₂S. In the present work, we have discovered that this wave (labeled as wave D in Figures 1 and 2c) is cleanly resolved from the bulk peak when using carefully annealed Ag(111) electrodes and slow voltammetric scan rates (<25 mV/s). Wave D has a half-wave potential of $E_{1/2} = -0.78 \text{ V vs Ag/AgCl}$ and is assigned to the oxidative formation of the second molecular layer of Ag₂S. The cathodic branch of wave D has an area equal to the anodic branch, indicating that the second monolayer of Ag₂S may be completely removed prior to removal of the first monolayer. In contrast to multistep deposition of the first monolayer, only one voltammetric wave is associated with the formation of the second monolayer. This is anticipated since adsorption of HS[−] to form an adlayer is not probable on a preexisting Ag₂S surface. The formation of the second monolayer is forced to occur in a one-step, two-electron process, eq 3.

From inspection of Figure 2c, it appears that the redox process associated with wave D is kinetically sluggish, as evidenced by the large potential peak splitting ($\sim 120 \text{ mV}$) between the anodic and cathodic waves. Growth of the second monolayer requires that either Ag⁺ be transported *outward* across the first Ag₂S monolayer, or that S^{2−} is transported *inward* toward the metal surface. For thicker Ag₂S films, it has been established that Ag⁺ migrates outward during film growth.²¹ Thus, the slow kinetics of wave D is most likely related to transport of Ag⁺ across the first Ag₂S monolayer.

It is interesting to note that the anodic peak of wave D, corresponding to the deposition of the second monolayer, occurs at potentials positive of the reversible potential for deposition of a bulk Ag₂S layer, E° . On thermodynamic grounds, wave D should not be observed since the bulk film is favored at potentials positive of E° . The reason that wave D is observed is that a large kinetic overpotential apparently exists for the formation of the bulk Ag₂S layer. Thus wave D is both energetically and kinetically resolved; waves C and D are resolved on the basis of the differences in energetics of formation of the first and second monolayers, while waves D and the “bulk” wave are separated on the basis of the differences in deposition kinetics of the second monolayer and bulk layer.

The coulometric charge associated with formation of the Ag₂S monolayers was estimated from the voltammetric data. To correct for the capacitive charging contribution, the area (proportional to the coulometric charge²²) enclosed in the background response (e.g., Figure 2a) was subtracted from the area enclosed under the voltammetric waves associated with formation of the first or second monolayers, Figure 2c. Half of the remaining value was taken to be the charge associated with the formation of the monolayers (this procedure eliminates the

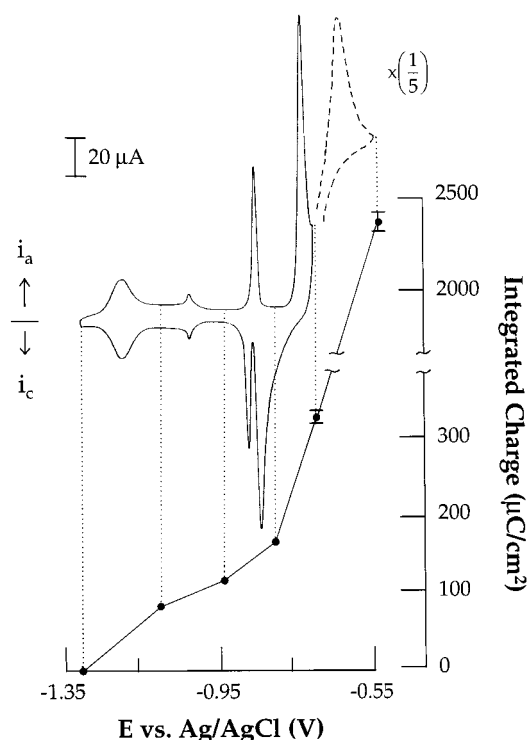


Figure 3. Integrated charge density ($\mu\text{C}/\text{cm}^2$) as a function of the electrode potential in a 0.2 M NaOH solution containing 1 mM Na₂S. (As a zero-order correction to account for non-Faradaic contributions, the charge density measured in a solution containing only the supporting electrolyte (0.2 M NaOH) has been subtracted from the corresponding values measured in the presence of HS⁻.) Integrated charges are averaged values obtained from eight independent measurements using different electrodes (except for the bulk value at -0.55 V vs Ag/AgCl, which is the average of 3 electrodes). Error bars (1σ) are smaller than the size of the data points, with the exception of the values at -0.70 and -0.55 V vs Ag/AgCl.

arbitrary decision of how to draw the capacitive baseline). An analogous procedure was employed to obtain the charge associated with adsorption of HS⁻ (waves A and B only) and for the oxidative transition between Ag-SH and Ag₂S (wave C).²³ Using this procedure, we have determined charge densities of $113 \pm 4 \mu\text{C}/\text{cm}^2$ for waves A and B (combined), and $55 \pm 5 \mu\text{C}/\text{cm}^2$ for wave C. Thus, the formation of the first Ag₂S monolayer (waves A, B, and C) consumes a charge of $169 \pm 4 \mu\text{C}/\text{cm}^2$, in reasonable agreement, but slightly smaller than values previously reported by our laboratory⁵ ($\sim 206 \mu\text{C}/\text{cm}^2$) and by Aloisi et al.⁷ ($\sim 185 \mu\text{C}/\text{cm}^2$).²⁴

Integration of the area under wave D alone yields a charge of $164 \pm 9 \mu\text{C}/\text{cm}^2$, equal to the charge associated with formation of the first Ag₂S monolayer (i.e., waves A, B, and C combined, $169 \pm 4 \mu\text{C}/\text{cm}^2$). Thus, the same amount of charge is consumed during formation of the first and second monolayers of Ag₂S. This finding is illustrated in Figure 3, where the integrated charge density (after background correction) is plotted as a function of the electrode potential.

The two-step mechanism proposed above, eqs 1 and 2, suggests that the charge associated with formation of the Ag-SH layer (waves A and B) should be equal to the charge associated with the transformation from the Ag-SH adlayer to a monolayer of Ag₂S. Experimentally, we find that the charge associated with waves A and B ($113 \pm 4 \mu\text{C}/\text{cm}^2$) is approximately twice as large as that for wave C ($55 \pm 5 \mu\text{C}/\text{cm}^2$). This finding clearly suggests that some of the HS⁻ is converted to Ag₂S at potentials prior to wave C, a result that appears consistent with the mechanism proposed by Aloisi et

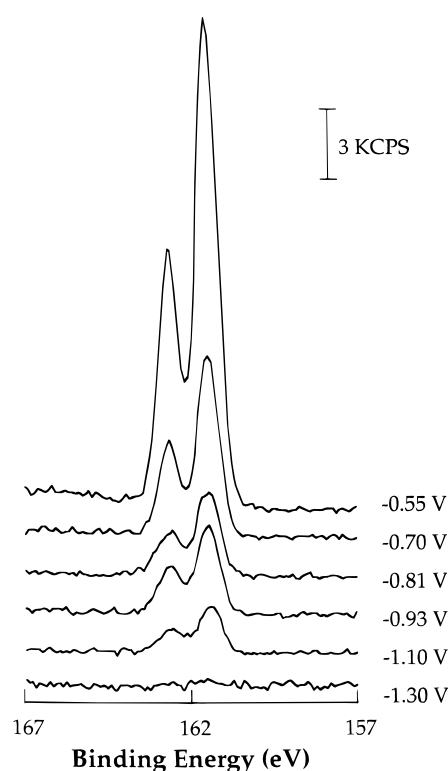


Figure 4. X-ray photoelectron spectra of Ag(111) electrodes removed from the HS⁻ solution as a function of the electrode potential. The peaks at 161.5 and 162.7 eV correspond to the 2p spin-orbit coupled 3/2 and 1/2 photoelectrons of S.

al.⁷ However, the XPS data presented below, as well as previous EQCM measurement of the adsorbed mass,⁵ demonstrate that no additional HS⁻ is adsorbed at the Ag(111) surface when the electrode potential is scanned through wave C. Therefore, it appears that neither our mechanism nor that of Aloisi et al.⁷ is entirely consistent with the experimental data. The fact that $\sim 2/3$ of the total charge associated with monolayer formation is accounted for by waves A and B (i.e., $113 \mu\text{C}/169 \mu\text{C} \approx 2/3$) suggests a possible energetic overlap of the two one-electron steps, eqs 1 and 2. For instance, both the adsorption of HS⁻ and oxidation of Ag-SH may contribute to the charge under wave B.

XPS was used to measure the surface coverage of S on the Ag(111) surface as a function of the electrode potential. The Ag(111) electrodes were removed from the HS⁻ solution *under potential control* by slowly lifting the wetted surface out of the solution. To ensure that no residual HS⁻ remains on the surface, the electrodes were thoroughly rinsed with a fine stream of triply distilled water directed at the air/solution interface as the electrodes were removed from the solution. This procedure prevents the spontaneous oxidation of Ag to Ag₂S when the electrode is exposed to air. The electrodes were then dried under a stream of N₂.

XPS spectra of the S 2p region as a function of the electrode potential are shown in Figure 4. The S 2p spectrum obtained at -1.30 V vs Ag/AgCl indicates that very little, if any, HS⁻ is adsorbed at potentials negative of wave A. The intensities of the XPS peaks clearly increase as the electrode potential is shifted to positive values, corresponding to the expected increase in the surface coverage of S.

Figure 5 shows the variation in integrated area of the S peak during the stepwise formation of the Ag-SH adlayer, the first Ag₂S monolayer, the second Ag₂S monolayer, and the bulk Ag₂S film. The data points represent the averaged values of at least

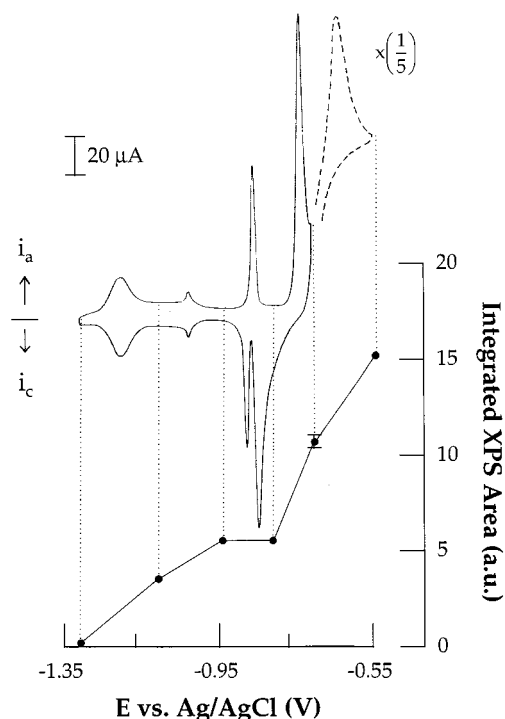


Figure 5. Integrated areas of the S 2p XPS peaks for Ag(111) electrodes removed from the HS[−] solution at different electrode potentials. Each data point represents the averaged values of five independent measurements using different Ag(111) electrodes. Error bars (1 σ) are smaller than the size of the data points, with the exception of the value at -0.70 V vs Ag/AgCl.

five independent measurements using different Ag(111) electrodes. With the exception of the data point at -0.70 V, the error bars are smaller than the size of the data points. As noted above, the XPS data indicate that S is not adsorbed onto the electrode surface at potentials that are negative of wave A. The area of the S 2p signal increases considerably upon scanning the electrode potential through waves A and B, consistent with the deposition of a Ag–SH adlayer. More significantly, the XPS data also indicate that no additional S is adsorbed over the course of wave C, in agreement with previous EQCM measurements.⁵ This is a key finding in that it strongly supports our proposed mechanism involving the surface phase transition, eq 2, between the Ag–SH adlayer and the Ag₂S monolayer.

When the electrode is removed from solution after scanning the potential through wave D, the area of the S signal increases nearly 2-fold. This increase is consistent with the formation of a second monolayer of Ag₂S. From the coulometric and XPS data, it appears that the charge and mass associated with the formation of the second Ag₂S monolayer is equivalent to that of the first monolayer. At potentials immediately following the fourth wave (D), bulk oxidation of the Ag electrode begins to occur and a relatively thick film of Ag₂S is formed (~ 15 monolayers). Over this potential range, the integrated S signal increases by only $\sim 50\%$. The relatively small increase in XPS signal is expected since photoelectron emission occurs only from the topmost layers.

Conclusion

The stepwise formation of the first and second molecular layers of Ag₂S at a Ag(111) electrode can be observed as well-defined waves in slow-scan voltammetric experiments. XPS and coulometric analysis indicate that the coverage and charge consumed, respectively, during the formation of the two layers

are nearly identical, suggesting that the first two monolayers are structurally similar. However, the finding that oxidative formation occurs at different electrode potentials clearly indicates that the free energies of formation of the first and second monolayers are significantly different. From an energetic point of view, the formation of the second monolayer is indistinguishable from the formation of bulk Ag₂S. However, deposition of the second monolayer during the voltammetric measurement can be resolved from growth of the bulk layer due to the kinetic overpotential for the latter process.

XPS analysis of the coverage of S on the Ag(111) electrode also supports the proposed mechanism for formation of the first Ag₂S monolayer. Specifically, the XPS data are consistent with a potential-dependent surface transition, eq 2, in which a Ag–SH adlayer is oxidized to a Ag₂S monolayer without increasing the total S surface coverage.

Acknowledgment. The assistance of Dr. Keith Stevenson in the preliminary steps of this work is gratefully appreciated. This work was supported by the Office of Naval Research. XPS analysis was performed using a National Science Foundation-funded surface analysis facility (CMS-9413498).

References and Notes

- (1) (a) Young, L. *Anodic Oxide Films*; Academic Press: New York, 1961. (b) Diggle, J. W. *Oxides and Oxide Films*; Dekker: New York, 1972. (c) *The Surface Science of Metal Oxides*; Henrich, V. E., Cox, P. A., Eds.; Cambridge: Great Britain, 1994. (d) Ajito, K.; Sukamto, J. P. H.; Nagahara, L. A.; Hashimoto, K.; Fujishima, A. *J. Electroanal. Chem.* **1995**, *386*, 229. (e) Wang, J.-R.; Wei, G.-L. *J. Electroanal. Chem.* **1995**, *390*, 29. (f) Czirok, E.; Bacskai, J.; Kulesza, P. J.; Inzelt, G.; Wolkiewicz, A.; Miecznikowski, K.; Malik, M. A. *J. Electroanal. Chem.* **1996**, *405*, 205. (g) *Electrochemical Synthesis and Modification of Materials*; Andricacos, P. C., Corcoran, S. G., Delplanck, J.-L., Moffat, T. P.; Searson, P. C., Eds.; Materials Research Society: Pittsburgh, Pennsylvania, 1997. (h) Bojinov, M.; Kanazirski, I.; Girginov, A. *J. Electroanal. Chem.* **1997**, *431*, 117.
- (2) (a) Larkin, D.; Guyer, K. L.; Hupp, J. T.; Weaver, M. J. *J. Electroanal. Chem.* **1982**, *138*, 401. (b) Salaita, G. N.; Lu, F.; Laguren-Davidson, L.; Hubbard, A. T. *J. Electroanal. Chem.* **1987**, *229*, 1. (c) Jaya, S.; Prasada Rao, T.; Prabhakara Rao, G. *J. App. Electrochem.* **1987**, *17*, 635. (d) Jovic, B. M.; Jovic, V. D.; Dracic, D. M. *J. Electroanal. Chem.* **1995**, *399*, 197. (e) Sneddon, D. D.; Gewirth, A. A. *Surf. Sci.* **1995**, *343*, 185. (f) Stevenson, K. J.; Gao, X.; Hatchett, D. W.; White, H. S. *J. Electroanal. Chem.* **1998**, *447*, 43.
- (3) The underpotential deposition (upd) of a monolayer of a foreign metal onto a metal electrode is analogous to the oxidative adsorption of an anion. In the upd process, reductive adsorption of the foreign metal occurs at electrode potentials positive of the standard potential of deposition of a bulk layer.
- (4) Hatchett, D. W.; White, H. S. *J. Phys. Chem.* **1996**, *100*, 9854.
- (5) Hatchett, D. W.; Gao, X.; Catron, S. W.; White, H. S. *J. Phys. Chem.* **1996**, *100*, 331.
- (6) The second one-electron step and corresponding surface phase transformation of the Ag–SH structure to the Ag₂S monolayer occurs at the Ag(110) and Ag(111) surfaces, but not at the Ag(100) surface. See ref 4 for further details.
- (7) Aloisi, G. D.; Cavallini, M.; Innocenti, M.; Foresti, M. L.; Pezzatini, G.; Guidelli, R. *J. Phys. Chem.* **1997**, *101*, 4774.
- (8) (a) Kimizuka, N.; Itaya, K. *Faraday Discuss.* **1992**, *94*, 117. (b) Bittner, A. M. *J. Electroanal. Chem.* **1997**, *431*, 51.
- (9) (a) Ogaki, K.; Itaya, K. *Electrochim. Acta* **1995**, *40*, 1249. (b) Chabala, E. D.; Ramadan, A. R.; Brunt, T.; Rayment, T. *J. Electroanal. Chem.* **1996**, *412*, 67. (c) Corcoran, S. C.; Chakarova, G. S.; Sieradski, K. *J. Electroanal. Chem.* **1994**, *377*, 85.
- (10) Polewska, W.; Wang, J. X.; Ocko, B. M.; Adzic, R. R. *J. Electroanal. Chem.* **1994**, *376*, 41.
- (11) (a) Biegler, T. *J. Electroanal. Chem.* **1963**, *6*, 357. (b) Biegler, T. *J. Electroanal. Chem.* **1963**, *6*, 365. (c) Biegler, T. *J. Electroanal. Chem.* **1963**, *6*, 373. (d) Stevenson, K. J.; Mitchell, M.; White, H. S. *J. Phys. Chem.* **1998**, *102*, 1235.
- (12) (a) Kolthoff, I. M.; Miller, C. S. *J. Am. Chem. Soc.* **1941**, *63*, 1405. (b) Fleischmann, M.; Rajagopalan, K. S.; Thirsk, H. R. *Trans. Faraday Soc.* **1963**, *59*, 741. (c) Bewick, A.; Fleischmann, M.; Thirsk, H. R. *Trans. Faraday Soc.* **1962**, *58*, 2200.

- (13) (a) Julien, L.; Bernard, M. L. *Rev. Chim. Min.* **1968**, *5*, 521. (b) Canterford, D. R.; Buchanan, A. S. *J. Electroanal. Chem.* **1973**, *45*, 193. (c) Zhdanov, S. I.; Kiselev, B. A. *Dokl. Akad. Nauk SSSR* **1964**, *155*, 651.
- (14) Fleischmann, M.; Thirsk, H. R. *Electrochim. Acta* **1964**, *9*, 757.
- (15) Armstrong, R. D.; Porter, D. F.; Thirsk, H. R. *J. Phys. Chem.* **1968**, *72*, 2300.
- (16) Stevenson, K. J.; Hatchett, D. W.; White, H. S. *Langmuir* **1996**, *12*, 494.
- (17) (a) Hatchett, D. W.; Stevenson, K. J.; Lacy, W. B.; Harris, J. M.; White, H. S. *J. Am. Chem. Soc.* **1997**, *119*, 6596. (b) Stevenson, K. J.; Hatchett, D. W.; White, H. S. *J. Israel Chem.* **1997**, *37*, 173. (c) Hatchett, D. W.; Uibel, R. H.; Stevenson, K. J.; Harris, J. M.; White, H. S. *J. Am. Chem. Soc.* **1998**, *120*, 1062.
- (18) Stevenson, K. J.; Hatchett, D. W.; White, H. S. *Langmuir* **1997**, *13*, 6824.
- (19) (a) Giggenbach, W. *Inorg. Chem.* **1971**, *10*, 1333. (b) Meyer, B.; Ward, K.; Koshlap, K.; Peter, L. *Inorg. Chem.* **1983**, *22*, 2345. (c) Myers, R. J. *J. Chem. Educ.* **1986**, *63*, 687. (d) Licht, S.; Longo, K.; Peramunage, D.; Forouzan, F. *J. Electroanal. Chem.* **1991**, *318*, 111.
- (20) E^0 is the standard potential for reaction 3 in the text, where all species correspond to bulk solids or species at unit activity in bulk solutions. E^0 was calculated on the basis of the reaction of $\text{Ag}^+ + e^- \rightleftharpoons \text{Ag}$, in equilibrium with the dissolution of Ag_2S ($\text{Ag}_2\text{S} \rightleftharpoons 2\text{Ag}^+ + \text{S}^{2-}$) and the dissociation of HS^- ($\text{HS}^- \rightleftharpoons \text{H}^+ + \text{S}^{2-}$). A value of 6.69×10^{-50} was

used as the solubility product, K_{sp} , of Ag_2S (*Handbook of Chemistry and Physics*; Lide, D. R., Ed.; CRC Press: Boca Raton, FL, 1991). A value of 16.9 was used as the $\text{p}K_{\text{a}}$ of HS^- .^{16d}

(21) (a) Wagner, C. Z. *Phys. Chem.* **1933**, *21B*, 25. (b) Uhlig, H. H.; Revie, R. W. *Corrosion and Corrosion Control*; Wiley: New York, 1985.

(22) The coulometric charge density is computed from $Q/A = \text{area}/(\nu \cdot X \cdot Y) \cdot A$, where Q is the coulometric charge (coul), A is the electrode area (cm^2), area is the integrated area of the voltammetric response (cm^2), ν is the potential scan rate (V/s), X is the potential axis scale (V/cm), and Y is the current axis scale (A/cm).

(23) The voltammetric curve shown in Figure 2a was used as the capacitive contribution for the curve in Figure 2c. To obtain the capacitive contribution for the potential range of waves A, B, and C, a similar background response was recorded in 0.2 M NaOH, covering only the necessary potential region (-1.30 to -0.80 V vs Ag/AgCl). A background curve recorded in 0.2 M NaOH covering the potential range of -1.30 to -0.93 V vs Ag/AgCl was used as the capacitive contribution for waves A and B.

(24) Hatchett et al.⁵ reported values of $114 \mu\text{C}/\text{cm}^2$ for waves A and B and $92 \mu\text{C}/\text{cm}^2$ for wave C. Likewise, Aloisi et al.⁷ reported values of 130 and $55 \mu\text{C}/\text{cm}^2$ for the corresponding waves, respectively. We believe that these coulometric charges have a slight degree of error associated with them that can be attributed to the roughness of the electrodes.